Molecular Neurobiology (2019) 56:6184–6196
https://doi.org/10.1007/s12035-019-1502-9

Microglial Depletion with Clodronate Liposomes Increases Proinflammatory Cytokine Levels, Induces Astrocyte Activation, and Damages Blood Vessel Integrity

Xiaoning Han[1] · Qian Li[1,2,3] · Xi Lan[1] · Leena EL-Mufti[1] · Honglei Ren[1] · Jian Wang[1]

Received: 13 December 2018 / Accepted: 18 January 2019 / Published online: 8 February 2019

Abstract

Investigators are increasingly interested in using microglial depletion to study the role of microglia under pathologic conditions. Liposome-encapsulated clodronate is commonly used to eliminate macrophage populations because it causes functionally irreversible inhibition and apoptosis once phagocytized by macrophages. Recent studies have shown that microglia can be depleted in disease models by injecting clodronate liposomes into the brain parenchyma. However, it is unclear whether intracerebral administration of clodronate liposomes is a practical method of eliminating microglia under physiologic conditions or whether microglial depletion induces damage to other brain cells. In this study, injecting 1 μL of clodronate liposomes (7 μg/μL) into the striatum of mice caused ablation of microglia at 1 day that persisted for 3 days. Microglia reappeared in the boundary regions of microglia elimination after 5 days. Importantly, we observed an increase in proinflammatory cytokine levels and an increase in neural/glial antigen 2 and glial fibrillary acidic protein expression in the perilesional region. In contrast, expression levels of myelin basic protein, microtubule-associated protein 2, and postsynaptic protein-95 decreased in the periphery of regions where microglia were depleted. Moreover, clodronate liposome administration decreased the density and integrity of blood vessels in the perilesional regions. In cultured primary neurons, clodronate liposome exposure also attenuated ATP synthesis. Together, these findings suggest that intracerebral administration of clodronate liposomes into brain parenchyma can deplete microglia, but can also damage other brain cells and blood vessel integrity.

Keywords Microglial depletion · Clodronate liposomes · Inflammation

Introduction

Clodronate, a member of the bisphosphonate family, is best known as an effective clinical therapy for osteometabolic disorders such as osteoporosis, arthritis, and osteo-articular pain [1–4]. When liposome-encapsulated clodronate (clodronate liposomes or Clo-Lip) is injected into an organ, it is phagocytosed by mononuclear phagocytes and then digested by lysosomal enzymes. Free clodronate then accumulates within the cytoplasm and induces apoptosis when the concentration exceeds a certain threshold [5–7]. Given a several-minute half-life in blood, free clodronate is rapidly cleared by the kidneys. Compared to several other chemicals that are able to deplete macrophages acutely, clodronate is used most frequently because of its high efficacy and minimal cytotoxicity [8].

Clo-Lip can be applied in multiple organs with different routes of administration [9]. It is a commonly used to investigate the role of macrophages in disease pathogenesis. Macrophages are central effector cells of the innate immune system that can initiate immune reactions and regulate the activity of other immunocytes. In general, the unhindered accessibility of Clo-Lip to reach a macrophage determines the efficacy of macrophage depletion.

Electronic supplementary material The online version of this article (https://doi.org/10.1007/s12035-019-1502-9) contains supplementary material, which is available to authorized users.

✉ Jian Wang
jwang79@jhmi.edu

[1] Department of Anesthesiology/Critical Care Medicine, School of Medicine, Johns Hopkins University, Baltimore, MD 21205, USA

[2] Present address: Department of Biochemistry and Molecular Biology, School of Basic Medical Sciences, Capital Medical University, Beijing 100069, People's Republic of China

[3] Present address: Advanced Innovation Center for Human Brain Protection, Capital Medical University, Beijing 100069, People's Republic of China

Thus, the predominant application of Clo-Lip is to deplete macrophages in the spleen, liver, and bone marrow through a circulatory route of administration.

In the brain, resident microglia, together with perivascular and meningeal macrophages, are generated from embryonic yolk sac precursors and constitute 10% of all brain cells [10, 11]. These immune cells defend against various neurologic diseases by secreting proinflammatory cytokines, interacting with astrocytes through chemokines, regulating oligodendrocyte remyelination, and affecting homeostatic maintenance of synapses and the blood-brain barrier [12–15]. The complex contributions to neuroinflammation distinguish microglia in the brain from blood monocyte-derived macrophages. Additionally, the cell types differ with respect to origin, rapidity of activation, and gene expression [16]. The changes associated with selective depletion of microglia by Clo-Lip have been examined in several studies. Nevertheless, no consensus exists on whether microglial depletion exacerbates or alleviates the basic pathology of primary brain injury in disease models. One study showed that depletion of activated microglia/macrophages reduced tumor metastasis [17]. In contrast, selective depletion of microglia induced hemorrhage and amplified local inflammation after acute ischemic stroke in the postnatal brain [18, 19], and perivascular macrophage depletion reduced amyloid clearance from the cerebral vasculature [20]. Clo-Lip was administered by either intracerebral or intraventricular injection in these studies. The different effects of microglial depletion might result from differences in disease models, animal species, animal age, or dosage and timing of clodronate administration.

Despite the controversial results of microglia/macrophage depletion after brain injury, these investigations demonstrated the feasibility of using Clo-Lip to deplete microglia. However, administration to the brain is potentially limited by the blood-brain barrier, astrocyte micro-anatomical domains, and neurovascular network. Thus, the following questions are raised. What is the efficacy of microglial depletion by Clo-Lip injection into the brain parenchyma? How is the large quantity of dead microglia cleared from the brain? Do other cell types survive the rapid die-off of the normally protective microglia? To determine whether microglial depletion by Clo-Lip is a practical approach to study the role of microglia in various brain injuries, we assessed the viability of other brain cells after Clo-Lip administration into the striatum of normal animals.

Materials and Methods

Animals

C57BL/6 male mice (8 to 10 weeks old, 23–25 g) were purchased from Charles River Laboratories (Frederick, MD). $Cx3cr1^{GFP/+}$ mice on C57BL/6 background (male, 8 to 10 weeks old, 23–25 g) obtained from Dr. Jonathan Bromberg (University of Maryland, Baltimore, MD) were used for visualization of microglia. All experimental procedures followed the STAIR and RIGOR guidelines and were approved by the Institutional Animal Care and Use Committee at Johns Hopkins University School of Medicine. Our reporting is compliant with the ARRIVE guidelines (http://www.nc3rs.org.uk/arrive). A total of 185 mice were used without death or exclusion. Animals were randomly assigned to different study groups by using the randomizer form at http://www.randomizer.org [21, 22]. Sample size calculations were based on our pilot studies. Investigators (XL and LE) blinded to the treatment groups evaluated outcomes in all mice and performed analyses.

Liposome Treatment

Clophosome-A clodronate liposomes (Anionic, 7 mg/mL, F70101C-A) and fluorescent Dil control liposomes (Dil-Lip; 0.14 mg/mL, F70101F-A) were purchased from FormuMax (Sunnyvale, CA, USA). Another batch of Clo-Lip (CP-005-005, 5 mg/mL) purchased from Liposoma (Amsterdam, The Netherlands) was used to confirm the efficiency of microglial depletion. The striatum was targeted because it is the brain region mostly affected by stroke models. $Cx3cr1^{GFP/+}$ mice and C57BL/6 mice were administered 1 μL of Clo-Lip or 1 μL of control Dil-Lip by injection into the left striatum (0.8 mm anterior and 2.0 mm lateral of the bregma, 3.0 mm in depth) as previously reported [21]. Another group received left lateral ventricle injections at 0.2 mm anterior and 0.8 mm lateral of the bregma, 2.0 mm in depth [23, 24]. Sham-operated mice underwent the same protocol, including needle insertion, but without liposome injection. Rectal temperature was monitored and maintained at 37.0 ± 0.5 °C by the DC Temperature Controller (FHC Inc., Bowdoin, ME) throughout the experimental and early recovery periods. Body weights were recorded before surgery and on days 1 and 3 after Clo-Lip injection.

Tissue Preparation and Histology

To track the cellular uptake of the liposomes, we observed the diffusion of Dil fluorescent dye under a fluorescence microscope on days 1 and 4 after injecting 1 μL of Dil-Lip into the striatum or lateral ventricle. Mice were perfused with phosphate-buffered saline (PBS) followed by 4% paraformaldehyde. Brains were post-fixed in 4% paraformaldehyde overnight at 4 °C and then transferred to 30% sucrose [25, 26]. Brains were cut with a vibratome

into 25-μm-thick coronal sections, spaced 200 μm apart, from rostral to caudal levels. Images were observed under a Nikon Eclipse 90i fluorescence microscope (excitation/emission = 550 nm/570 nm). The total diffusion distance was calculated as the number of sections with Dil-Lip multiplied by the distance between the sections (200 μm). To quantify the efficacy of microglial depletion, we treated $Cx3cr1^{GFP/+}$ mice with 1 μL Clo-Lip. Images were collected with a fluorescence microscope (Nikon Eclipse 90i, Japan) at constant parameters. Image J software (NIH, Image J 1.47 t) was used for analyzing images.

Flow Cytometry

Four 1-mm-thick sections of the left striatum were dissected from one $Cx3cr1^{GFP/+}$ mouse with a mouse brain slicer matrix (Zivic Instruments, Pittsburgh, PA), and microglia from three mice were isolated and pooled. The striatum was dissociated by magnetic-activated cell sorting with the GentleMACS Dissociator and Neural Tissue Dissociation Kit (Miltenyi Biotec) [27, 28]. Myelin was removed by incubating single-cell suspensions with anti-myelin immunoglobulin-conjugated magnetic microbeads (Myelin Removal Kit; Miltenyi Biotec). After the cells were washed, cell supernatants were analyzed by CytoFLEX (Beckman Coulter, Indianapolis, IN) with CytExpert software 2.0 (Beckman Coulter). Propidium iodide (Sigma, St. Louis, MO) staining was used to exclude dead cells. The GFP fluorochromes were excited with the 488-nm laser and GFP-positive cells were gated.

Immunohistochemistry

We stained 25-μm-thick coronal sections by standard immunohistochemistry procedures as previously described [29, 30]. Briefly, brain sections were permeabilized and blocked with 0.5% Triton X-100 and 10% normal goat serum in PBS for 1 h at room temperature and then incubated overnight at 4 °C in 0.1% Triton X-100 and 1% normal goat serum in PBS with primary antibodies. The primary antibodies for immunohistochemistry were anti-neural/glial antigen 2 (NG2; 1:400, AB5320, Millipore, Burlington, MA, USA), anti-CD68 (1:200, MCA1957, AbD Serotec, Hercules, CA, USA), anti-glial fibrillary acidic protein (GFAP; 1:500, G3893, Sigma), anti-myelin basic protein (MBP; 1:2000, SMI 94R-500, Biolegend, San Diego, CA, USA), anti-microtubule-associated protein 2 (MAP2; 1:5000, ab5392, Abcam, Cambridge, MA, USA), anti-postsynaptic density protein 95 (PSD95; 1:100, 36233, Cell Signaling Technology, Danvers, MA, USA), anti-neurofilament (1: 400, N0142, Sigma), and anti-CD31 (1:200; ab56299, Abcam). All fluorescent-conjugated secondary antibodies (Life Technologies, Grand Island, NY, USA) were used at a dilution of 1:1000. Nuclei were labeled with DAPI (1:1000, Life Technologies, R37606). Omission of the primary antibody was used as a negative control. Images were captured with a fluorescence microscope (Nikon Eclipse 90i) from five optical fields in each of five sections per animal. Image J software was used to analyze images from the region of interest. The average fluorescence intensity was expressed as a percentage of the intensity in the peri-injection region normalized to the contralateral side of the same section.

Primary Neuronal Culture and ATP Assay

Prenatal C57BL/6 pups were used to culture primary neurons as described previously [31]. Briefly, the cerebral cortex of pups was collected on embryonic days 15–17 under a microscope. The cells were isolated with 0.25% trypsin (Gibco, Grand Island, NY, USA) and plated with Neurobasal medium supplemented with B27, 2 mM glutamine, and streptomycin/penicillin (Life Technologies) onto 96-well tissue culture plates coated with poly-D-lysine (Sigma). Cells at 7–9 days in vitro were exposed to various concentrations of Dil-Lip or Clo-Lip. ATP was assayed (Lonza, Pittsburgh, PA, USA) in the cells at 18 h after liposome incubation according to the manufacturer's instruction [32]. The ATP level was determined in a luminometer microplate reader (Molecular Devices, San Jose, CA, USA). At least three independent experiments were performed.

Western Blot Analysis and ELISA

Four 1-mm-thick striatal slices were isolated (sagittal distance from bregma, 2.8 to − 1.2 mm) with a mouse brain slicer matrix (Zivic Instruments, Pittsburgh, PA, USA). Plasma membrane-associated proteins were extracted by T-PER reagent (Pierce, Dallas, TX, USA) with a complete mini protease inhibitor cocktail (Roche Molecular Biochemicals, St. Louis, MO, USA). Proteins were separated by sodium dodecyl sulfate-polyacrylamide gel electrophoresis and transferred onto polyvinylidene fluoride membranes [21, 33]. Membranes were incubated with primary antibodies against rabbit anti-zonula occludens-1 (ZO-1; 1:1000, 617300, Life Technologies) and mouse anti-claudin-5 (1:000, 352500, Life Technologies) at 4 °C overnight. β-Actin (1:3000, sc-47778, Santa Cruz Biotechnology, Dallas, TX, USA) was used as a loading control. Anti-rabbit or anti-mouse secondary antibody (Santa Cruz Biotechnology) was used at a dilution of 1:3000. Protein signals were visualized under an

ImageQuant ECL Imager (LAS-4000, GE Healthcare). Band intensities were quantified with Image J software. Optical density values were normalized to the corresponding loading control intensity and expressed as fold change.

The concentrations of proinflammatory cytokines (IL-1β, IL-6, and TNF-α) in 4-mm-thick striatal slices were measured by ELISA kits (R&D System, Minneapolis, MN, USA) [27] on days 1, 3, 5, and 7 after liposome injection. Four 1-mm-thick striatal slices were briefly isolated (sagittal distance from bregma, 2.8 to − 1.2 mm) with a mouse brain slicer matrix (Zivic Instruments, Pittsburgh, PA, USA). The brain tissue was then homogenized in T-PER reagent (Pierce, Dallas, Texas, USA), in which the homogenate was centrifuged at 13,000×*g* for 20 min. The supernatants were collected for ELISA assay.

Statistical Analysis

Data are presented as mean ± SD or mean ± SEM. Two-tailed Student's *t* test was used for comparisons between two groups. Differences among multiple groups were analyzed by one-way or two-way ANOVA with Bonferroni post hoc test. All analysis was carried out with SigmaPlot 12.5 software. A probability value of $p < 0.05$ was considered statistically significant.

Results

Clodronate Liposomes Deplete Striatal Microglia

To determine the optimal method of liposome dispersal, we injected 1 μL of fluorescent Dil-Lip into the striatum or lateral ventricle. At 24 h after striatal administration, Dil-Lip was detected in the striatum, and the maximum diffused distance from the anteroposterior ordinate was 3 mm (Fig. 1a). Only negligible amounts of Dil-Lip had spread from the ependymal wall at 24 h after left lateral ventricle injection (Fig. 1b). Diffusion from lateral ventricle injection was not improved even after we increased the volume of Dil-Lip to 5 μL (not shown) or extended the time to 4 days after injection (Supplementary Fig. 1a, b). Therefore, we chose to inject 1 μL of Clo-Lip into the striatum of Cx3cr1$^{GFP/+}$ mice. The mice did not exhibit obvious weight loss by 3 days after Clo-Lip treatment (Supplementary Fig. 1c). Contralateral striatum was used as a morphological control. Microglial depletion in the striatum was prominent at day 1 and lasted for 3 days after Clo-Lip injection. The number of microglia in the ipsilateral striatum as a percentage of that in the contralateral striatum was 70.9 ± 16.0% at day 1, 40.2 ± 11.6% at day 2, and 53.8 ± 17.9% at day 3 ($n = 3$–5 per group, $p < 0.01$). Dil-Lip did not cause significant microglial loss (Fig. 1c, d). We also observed that striatal Clo-Lip extended to the white matter and that microglia in corpus callosum were depleted on day 3 after striatal Clo-Lip injection (Fig. 1e). Together, these data indicate a continuous elimination of microglia in both gray and white matter after Clo-Lip injection into brain parenchyma.

Reappearance of Microglia in the Peri-injection Region

We used immunohistochemistry and flow cytometry to evaluate the efficiency with which Clo-Lip depleted microglia. We noted that in the ipsilateral striatum, Cx3cr1-GFP-positive microglia accumulated at the edge of the microglia-depletion zone at 5 days after Clo-Lip treatment. Some microglia were activated, as distinguished by the enlarged cellular diameter (> 7.5 μm), shorter processes, and CD68-positive immunostaining (Fig. 2a). The maximum diffusion distance on the ordinate was 3 mm by 1 μL of Clo-Lip. Thus, we dissociated 4-mm-thick sections of ipsilateral striatum and divided the cells into Cx3cr1-GFP-positive and Cx3cr1-GFP-negative populations by flow cytometry (Supplementary Fig. 1d). In accordance with our histological observations, flow cytometry revealed decreases in Cx3cr1-GFP-positive microglia in ipsilateral striatum at day 1 to 57.3 ± 5.7% and at day 4 to 62.0 ± 2.7%. Populations had recovered at day 7 to 96.9 ± 11.9% ($n = 3$–4 per group, Fig. 2b). In contrast, the number of Cx3cr1-GFP-positive cells in the ipsilateral cortex did not differ from that in the sham group at any time point (Fig. 2c and Supplementary Fig. 1e). An increase in NG2-positive cells has been hypothesized to induce glial cell differentiation and proliferation after brain insults. Therefore, we next assessed NG2 expression by immunohistochemistry. Clo-Lip treatment significantly upregulated NG2 expression in ipsilateral striatum at day 7 (Fig. 2d).

Clodronate Liposomes Upregulate Proinflammatory Cytokines and Activate Glia

To investigate whether microglial depletion induces brain injury, we first analyzed the concentrations of proinflammatory cytokines by ELISA. The levels of IL-1β, IL-6, and TNF-α were upregulated at days 1 and 3 after Clo-Lip injection ($n = 3$–10, $p < 0.01$; Fig. 3a) but had returned to baseline at day 5. The same volume of Dil-Lip did not induce a clear inflammatory response (Fig. 3a). We next evaluated the response of astrocytes and oligodendrocytes in the peri-injection area of mice. To exclude the mechanical injury induced by needle insertion, we carefully chose the area outside the injection core for imaging and analysis (Fig. 3b). GFAP expression was higher and MBP level lower in the ipsilateral striatum than in the contralateral striatum 7 days after Clo-Lip injection

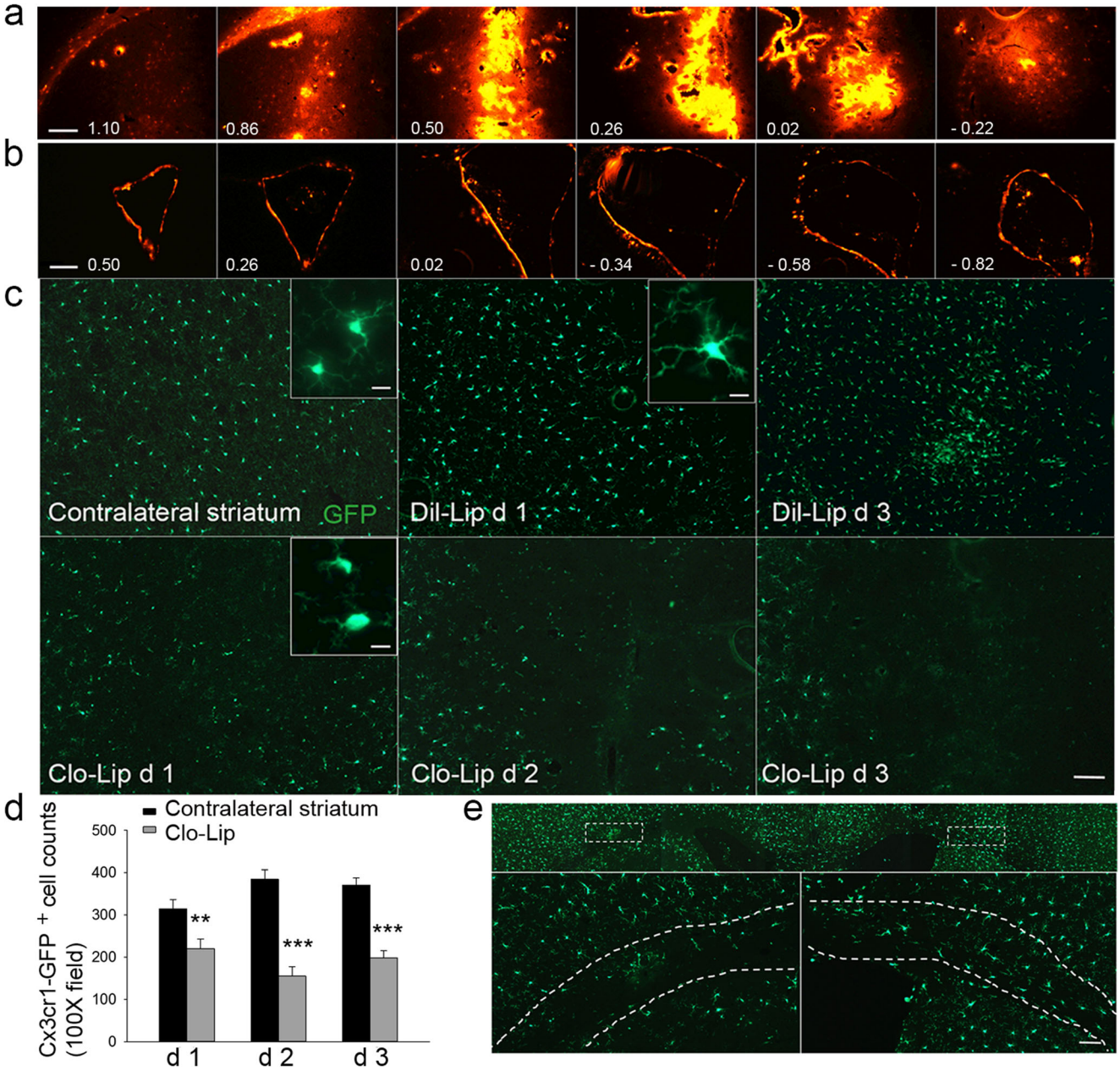

Fig. 1 Injection of clodronate liposomes (Clo-Lip) into brain parenchyma depletes microglia starting at 24 h. **a**, **b** Series of brain sections at day 1 after injection of 1 μL Dil-Lip (liposomes labeled with red fluorescent dye Dil) into striatum (**a**) or lateral ventricle (**b**). Numbers shown indicate anteroposterior ordinate distance to the bregma. Scale bar = 100 μm. **c** Representative images show depletion of Cx3cr1-GFP$^+$ microglia (green) at different time points after striatal injections with Dil-Lip or Clo-Lip. Insets show higher magnification images of microglia. Scale bar = 100 μm, inset, 10 μm. **d** Quantification of Cx3cr1-GFP$^+$ cells in striatum after 1 μL Clo-Lip injection. $n = 3$–5/group; $^{**}p < 0.01$, $^{***}p < 0.001$ versus contralateral striatum, two-way ANOVA with Bonferroni multiple comparison test. Data are presented as means ± SEM. **e** Representative images show that Cx3cr1-GFP$^+$ microglia (green) are depleted in corpus callosum (outlined) on day 3 after striatal Clo-Lip injection. Scale bar = 100 μm

(Fig. 3c, d). These data indicate that Clo-Lip induced an inflammatory reaction in the brain.

Clodronate Liposomes Induce Neuronal Degeneration

To evaluate the impact of microglial depletion on neuronal morphology and function, we assessed neuronal injury around the injection area on day 7 after Clo-Lip treatment. We also analyzed expression of MAP2, PSD95, and neurofilaments using immunohistochemistry. Contralateral striatum was used as a control. Microglial depletion reduced the expression of MAP2 to 74.8 ± 13.1% (Fig. 4a), PSD95 to 83.6 ± 14.3% (Fig. 4b), and neurofilament to 68.9 ± 22.1% (Fig. 4c) of contralateral levels. We further assessed neuronal function by

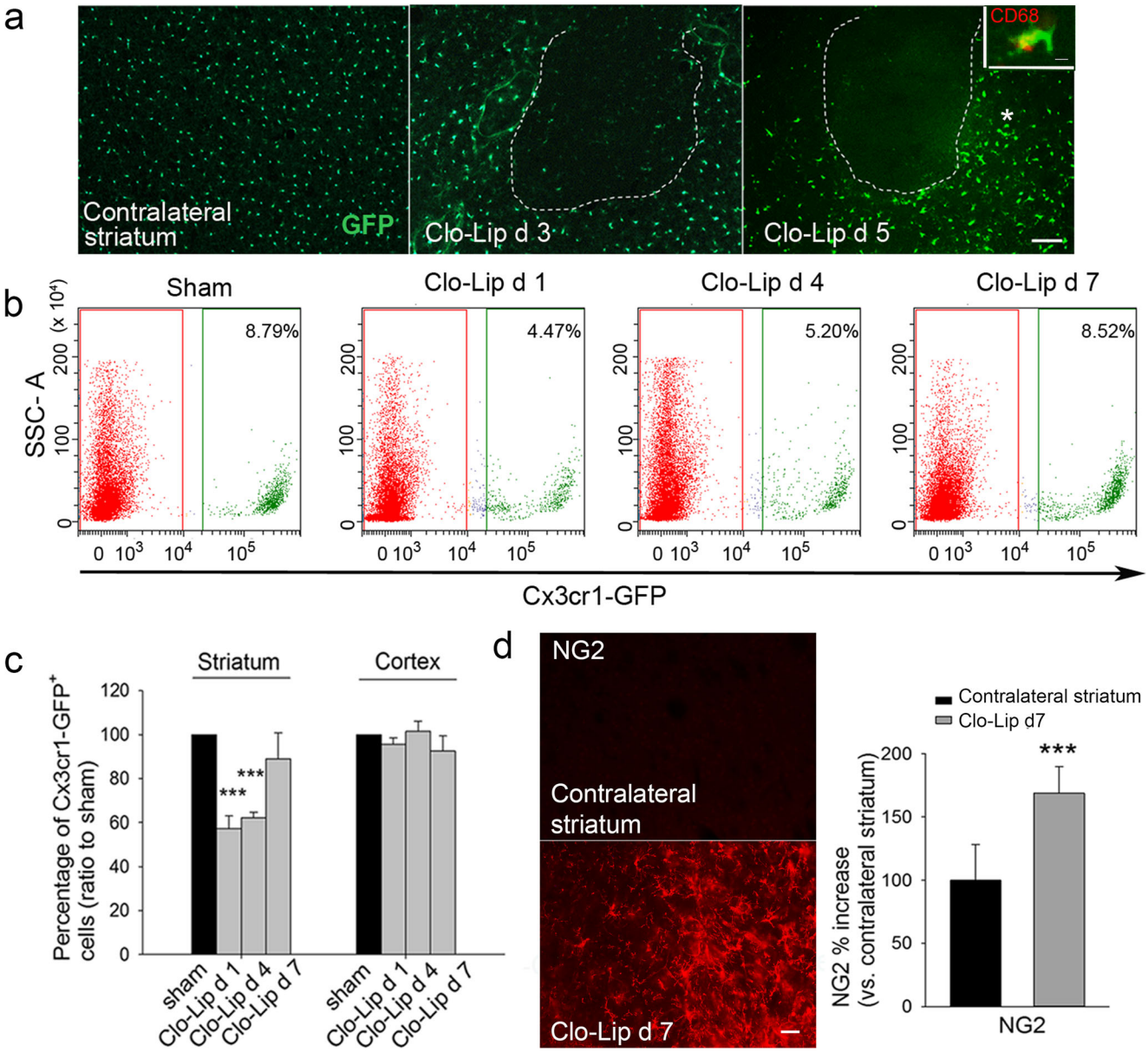

Fig. 2 Microglia reappear in the peri-injection region 5 days after striatal clodronate liposome (Clo-Lip) injection. **a** Representative images of Cx3cr1-GFP$^+$ microglia in striatum on days 3 and 5 after 1 μL Clo-Lip injection. The outlined areas indicate the sites of microglial depletion. Scale bar = 100 μm. Asterisk in the right image indicates the fields where microglia repopulated. Inset: high magnification of microglia around the outline, scale bar = 5 μm. Green, Cx3cr1-GFP; red, CD68. **b** Cx3cr1-GFP$^+$ microglia were analyzed by flow cytometry on days 1, 4, and 7 after Clo-Lip injection. Representative dot plots are shown, and the percentages of Cx3cr1-GFP$^+$ in the striatal cell population are indicated. Red, Cx3cr1-GFP$^-$ cell population; green, Cx3cr1-GFP$^+$ cell population. **c** Graphs show the percentage of remaining Cx3cr1-GFP$^+$ population in striatum and cortex after Clo-Lip injection. $n = 3$–4/group; $^{***}p < 0.001$ versus sham group; one-way ANOVA with Bonferroni post hoc test. Data are presented as means ± SD. **d** Representative images and quantification show that NG2-positive cells (red) increased in striatum at day 7 after Clo-Lip injection. Scale bar = 50 μm. $n = 5$; $^{***}p < 0.001$ versus contralateral striatum; Student's t test

ATP assay in primary cortical neuronal culture. Primary cultured mouse neurons were observed to endocytose Dil-Lip at various concentrations (Fig. 4d), but with no change in ATP content. In contrast, exposure of cultured neurons to Clo-Lip induced significant decreases in ATP (Fig. 4e). These data indicate that Clo-Lip-induced microglial depletion impairs neuronal function.

Microglial Depletion by Clodronate Liposomes Weakens Blood Vessel Integrity

To address whether microglial depletion damages blood-brain barrier integrity, we first evaluated the density and diameter of CD31-positive blood vessels around the injection region on day 7 after Clo-Lip

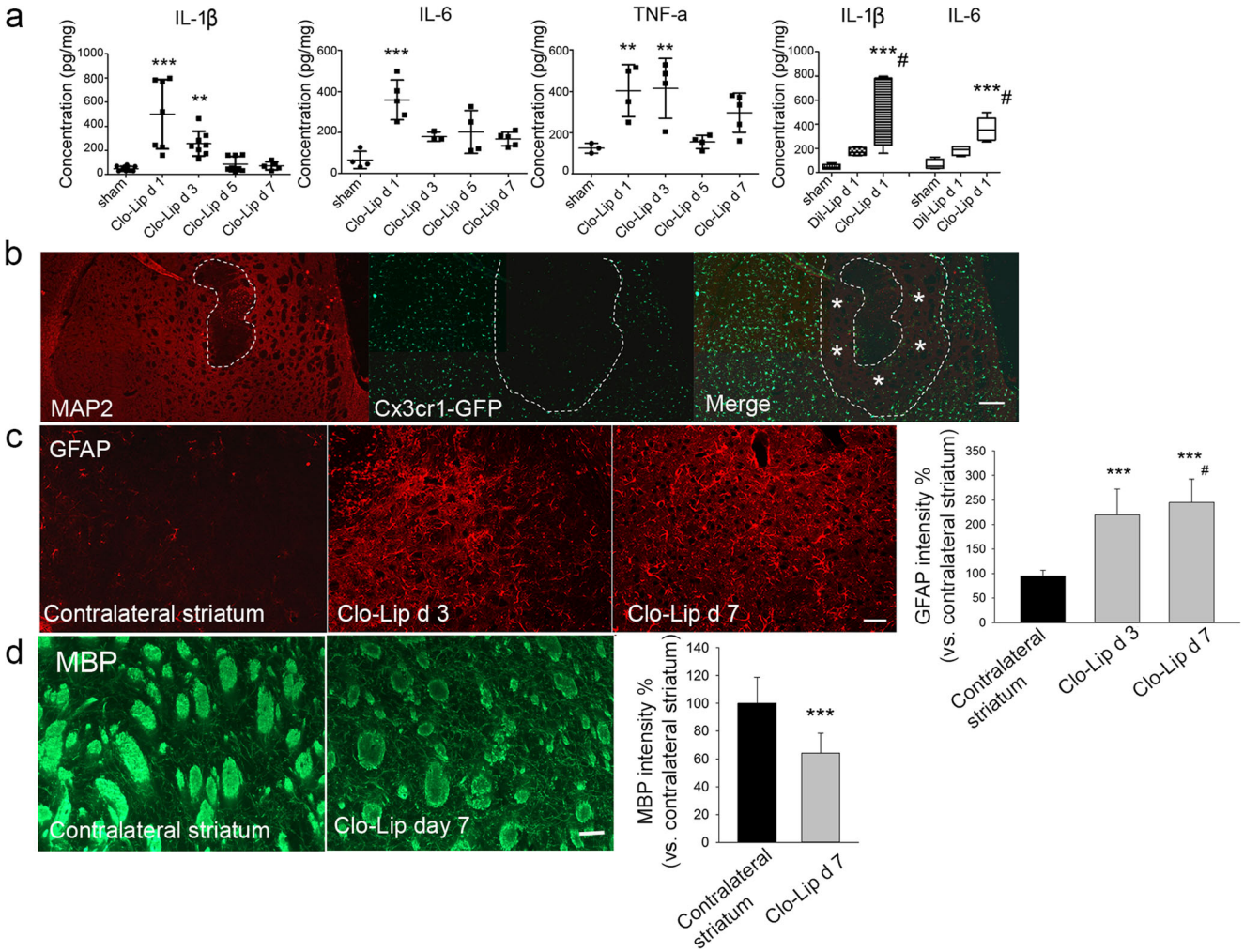

Fig. 3 Microglial depletion upregulates proinflammatory cytokine levels and induces astrocyte activation. **a** Concentrations of IL-1β, IL-6, and TNF-α in striatum were measured with ELISA on days 1, 3, 5, and 7 after injection of clodronate liposomes (Clo-Lip) or Dil-labeled liposomes (Dil-Lip). $n = 3$–10/group; e.g., $n = 3$ in the TNF-α sham group, $n = 10$ in the Dil-Lip d1 group; $^{**}p < 0.01$, $^{***}p < 0.001$ versus sham group; $\#p < 0.05$ versus Dil-Lip group; one-way ANOVA with Bonferroni post hoc test. Data are presented as means ± SD. Data in the last graph are presented as box-and-whisker plots. The middle horizontal line within the box represents the median, and boxes extend from the 5th to 95th percentile. **b** Low magnification images show the core injection (outlined in left panel) and region of microglial depletion (outlined in middle panel). Asterisks in the right image indicate the fields where the images in Figs. 3**c**, **d**, 4, and 5 were taken. Red, MAP2; green, Cx3cr1-GFP. Scale bar = 100 μm. **c** Representative images of glial fibrillary acidic protein (GFAP) expression (red) on days 3 and 7 after Clo-Lip injection. Scale bar = 50 μm. The graph shows the percent increase in GFAP. $n = 6$; $^{***}p < 0.001$ versus contralateral striatum group; $\#p < 0.05$ versus Clo-Lip day 3 group; one-way ANOVA with Bonferroni post hoc test. Data are presented as means ± SD. **d** Representative images and quantification show downregulation of myelin basic protein (MBP) at 7 days after Clo-Lip injection. $n = 6$; $^{***}p < 0.001$ versus contralateral striatum; Student's t test. Data are presented as means ± SD

administration. The density of blood vessels decreased, but blood vessel diameter was unaffected ($n = 6$, Fig. 5a, b). We further evaluated the expression of tight junction proteins claudin-5 and ZO-1 by immunoblotting. In sham-injected animals, claudin-5 was present as a band with a molecular weight of approximately 20 kDa. However, claudin-5 expression was upregulated as early as day 3 after Clo-Lip treatment and remained elevated through day 7 (bands at 20 kDa, $n = 6$, $p < 0.001$; Fig. 5c). Microglial depletion did not alter ZO-1 expression on days 1 or 3 ($n = 6$, $p = 0.25$; Fig. 5d). These data indicate that injury to the blood-brain barrier cannot be ruled out.

Discussion

In this study, a single intracerebral injection of Clo-Lip effectively depleted parenchymal microglia. Clo-Lip also depleted microglia in the white matter along the needle track.

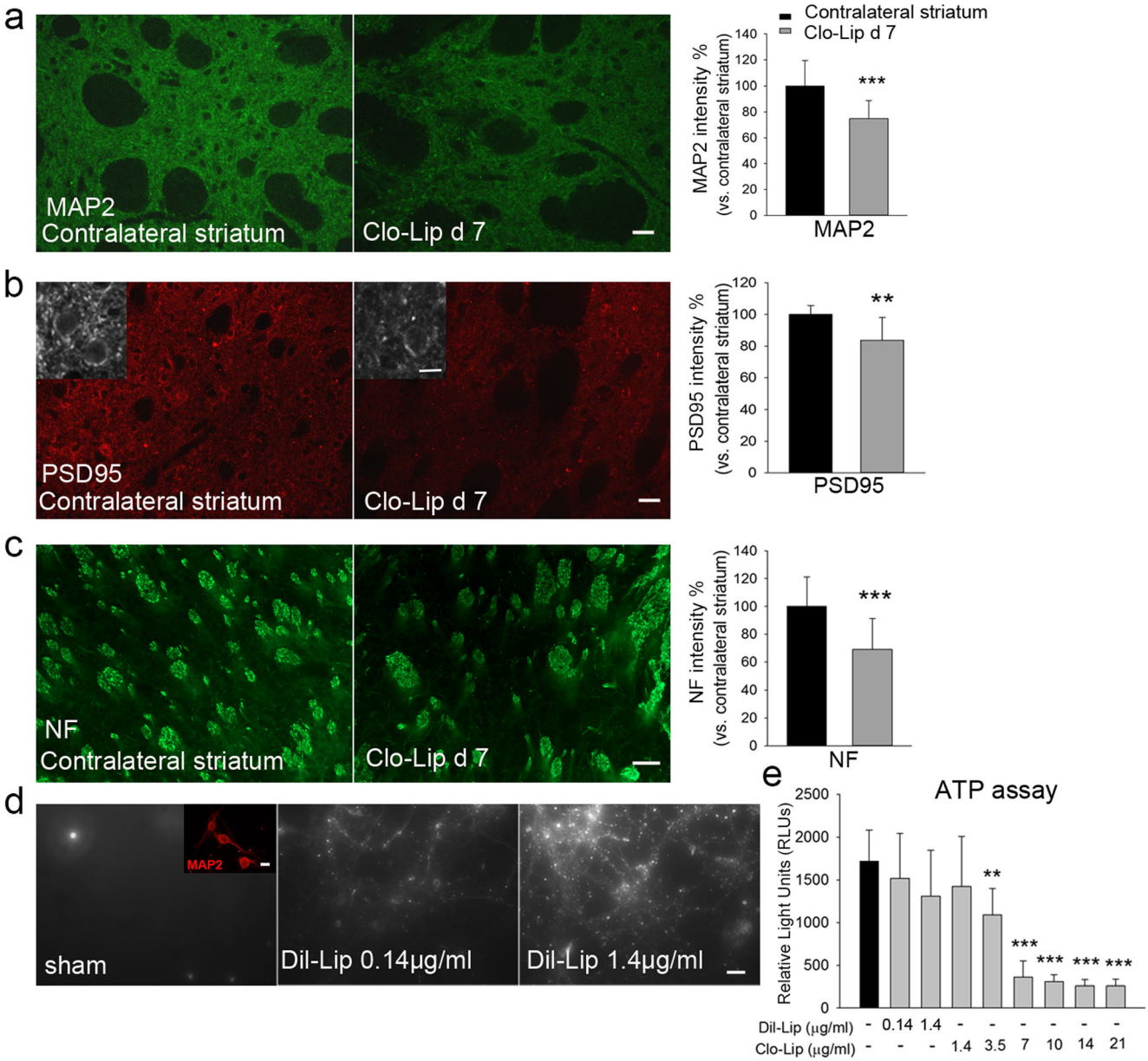

Fig. 4 Microglial depletion induces neuronal degeneration. **a**–**c** Representative images and quantification of MAP2 (green, **a**), PSD95 (red, **b**), and neurofilament (NF; green, **c**) expression on day 7 after clodronate liposome (Clo-Lip) injection. Scale bars: **a** 25 μm; **b** 25 μm, inset 10 μm; **c** 50 μm. $n = 6$ per group; $^{**}p < 0.01$, $^{***}p < 0.001$ versus contralateral striatum; Student's *t* test. **d** Representative images of primary cultured neurons exposed to Dil-labeled liposomes (Dil-Lip) for 18 h. Inset: high magnification of cultured neurons with MAP2 immunofluorescence staining. White, Dil-Lip. Red, MAP2. Scale bar = 25 μm; inset, 10 μm. **e** Primary cultured neurons were exposed to different concentrations of Dil-Lip or Clo-Lip for 18 h. Then cytotoxicity of neurons was measured by ATP assay. $n = 8$–12 ($n = 8$ in the sham group, $n = 12$ in other groups). $^{**}p < 0.01$, $^{***}p < 0.001$ versus sham group; one-way ANOVA with Bonferroni post hoc test. Data are presented as means ± SD

Repopulation of microglia began 5 days after administration. Microglia in the striatum were reduced by up to 49% in four successive 1-mm-thick slices of left striatum with one 7-μg dose of Clo-Lip, much less than that used in previous investigations. Higher doses would be needed for complete depletion of microglia. Notably, however, selective microglial depletion by Clo-Lip induced concurrent injury to other types of brain cells.

Our findings indicate that intracerebral injection of Clo-Lip is an effective route for depleting parenchymal microglia, in accordance with the results of others [18, 19]. Although intraventricular injection has been reported to deplete perivascular

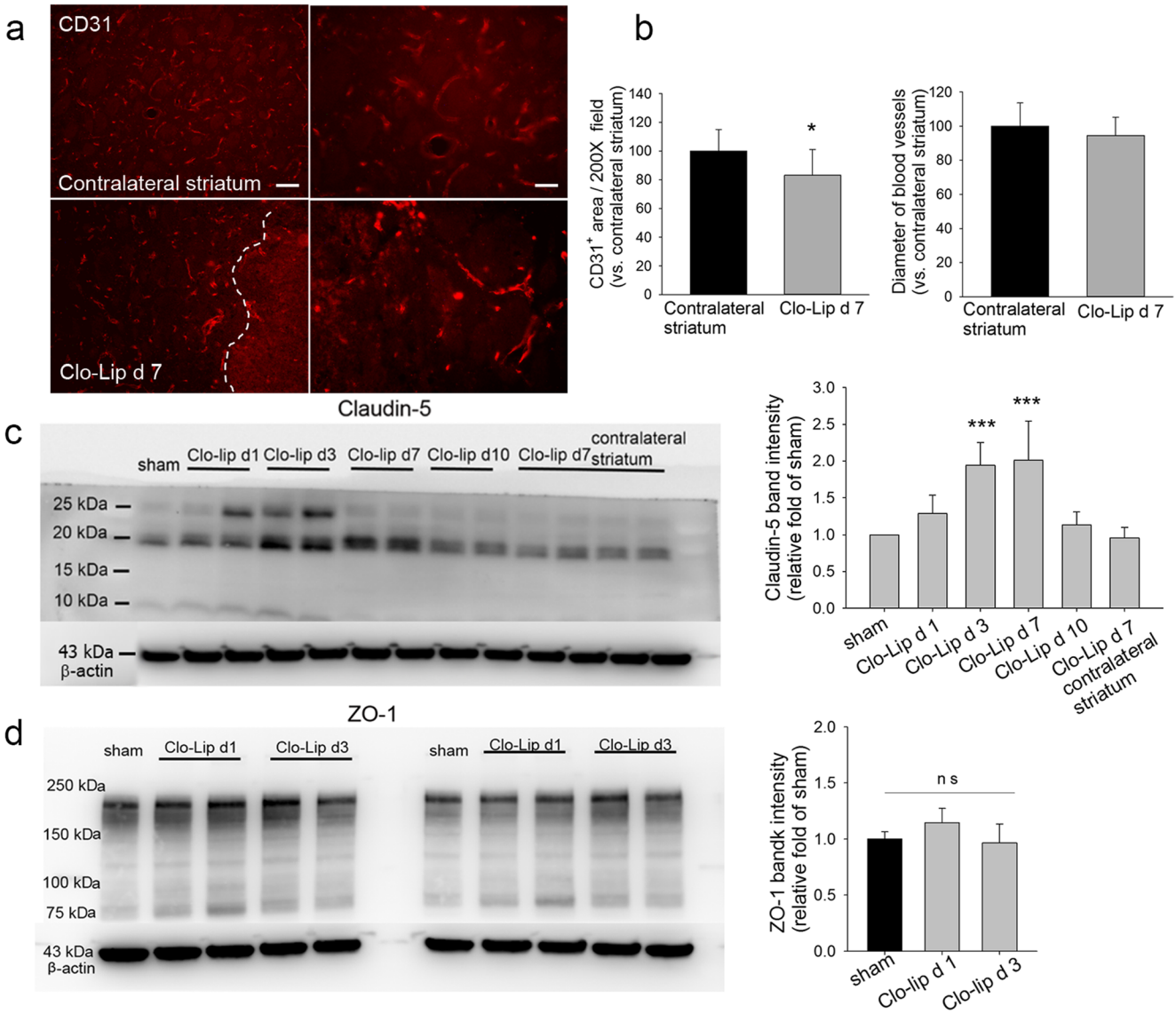

Fig. 5 Microglial depletion reduces the density and integrity of blood vessels. **a** Left panel, representative images of CD31 expression (red) on day 7 after Clo-Lip injection. Outlined area indicates injection center. Right panel, higher magnification images of CD31. Scale bars = 50 μm (left panel), 25 μm (right panel). **b** The density and diameter of blood vessels. $n = 6$; $^{*}p < 0.05$; unpaired Student's t test. Data are presented as means ± SD. **c** Degraded claudin-5 was analyzed by Western blot at each time point after Clo-Lip injection. Claudin-5 (MW, 20 kDa) was increased on days 3 and 7 after Clo-Lip injection. $n = 6$; $^{***}p < 0.001$ versus sham group; one-way ANOVA with Bonferroni post hoc test. Data are presented as means ± SD. **d** Expression of ZO-1 on days 1 and 3 after Clo-Lip injection. $n = 6$; ns, not significant. One-way ANOVA with Bonferroni post hoc test. Data are presented as means ± SD

and meningeal macrophages [20, 34], we found this route to be ineffective for eliminating microglia in adult brain. A recent study indicated that PLX5622, a colony-stimulation factor 1 receptor (CSF1R) inhibitor, induced selective microglial ablation without upregulating inflammation-related genes when administered in the diet for 14 days. Subsequent microglial repopulation occurred by proliferation of residual microglia after 99% of microglia were ablated [35]. However, our results suggest that some newly appeared or accumulated microglia might be activated inflammatory microglia after Clo-Lip injection (7 μg/1 μL), consistent with the enlarged somas and CD68 expression. The time course of microglial repopulation and changes of cell morphology, distribution, and maturation status may vary with the percentage of microglia that are depleted. Moreover, contrary to previous studies, microglial elimination in striatum increased the levels of proinflammatory cytokines at days 1 and 3 after Clo-Lip injection [18, 19]. The differing results are likely associated with the different routes of administration or ages of animals.

Although the upregulated proinflammatory cytokines in the ipsilateral striatum returned to baseline at day 5 after Clo-Lip injection, microglial depletion affected the function

of other brain cell types for at least 7 days. GFAP was increased from day 3 to at least day 7. Degenerating neurons and oligodendrocytes exhibited decreased MAP2, PSD95, and MBP. Clodronate in the cytoplasm can be metabolized to an analog of ATP and translocated into the mitochondria, where it blocks the respiratory chain by inhibiting ADP/ATP translocase, initiating cell apoptosis [36, 37]. This is likely the mechanism by which Clo-Lip induces macrophage apoptosis. Lysosomes in neurons are abundant in the soma, moderately frequent in dendrites, and relatively rare in axons. These endocytotic lysosomes are relevant to neuronal physiology and pathophysiology [38–40]. For example, AMPA-type glutamate receptors at the postsynaptic surface can be endocytosed and degraded by lysosomes or reinserted into the membrane for recycling. This balance is critical for synaptic plasticity [41, 42]. In Alzheimer's disease, the swollen axons surrounding amyloid plaques are enriched with lysosomes [43, 44]. Because neurons contain numerous lysosomes and neuronal activities require ATP synthesis [45], we asked whether Clo-Lip can be metabolized by neuronal lysosomes and thereby affect the function of neurons directly. Interestingly, our analysis showed that Clo-Lip suppressed the ATP synthesis in primary cultured neurons. Whether Clo-Lip accesses primary cultured neurons by endocytosis needs to be investigated.

Our data also revealed that microglial depletion damaged the integrity and density of blood vessels. However, Fernandez-Lopez et al. [18] reported previously that intracerebral administration of Clo-Lip to neonatal rats did not affect the blood-brain barrier when compared to that on the contralateral side, which was injected with PBS-liposomes. This difference in findings might be due to differences in blood-brain barrier functional integrity between neonates and adults [46]. Microglia are thought to maintain the integrity of the blood-brain barrier and neuronal synapses in adults [12, 13]. Our data have indicated the presence of secondary damage to neurons and endothelial cells after microglial elimination under physiologic conditions.

An increase in NG2-positive cells (polydendrocytes) is associated with activation of astrocytes and microglia/macrophages and influences proliferation and migration of oligodendrocyte precursor cells [47–49]. NG2-positive cell-derived microglia and astrocytes can be detected after central nervous system injuries such as spinal cord injury, experimental autoimmune encephalomyelitis, and an ischemic stroke model [50, 51]. Our data showed that many NG2-positive cells appeared in the ipsilateral striatum at 7 days after Clo-Lip administration. Whether these NG2-positive cells contribute to the repopulation of microglia or activated astrocytes needs further investigation.

Prior studies have shown that Clo-Lip administration in vitro improves the purity of cultured astrocytes and increases the frequency of excitatory postsynaptic current in organotypic hippocampal slice cultures [52, 53]. These studies indicated that microglial elimination does not affect the viability or activation of astrocytes. Thus, Clo-Lip might be applicable to in vitro studies because, unlike application in the brain, even if Clo-Lip is cytotoxic to other cells, the toxicity might be diminished by changes in culture medium.

Methods for eliminating microglia are still being developed. Transgenic mice in which a key microglial protein is knocked out or functionally blocked have been utilized for some investigations. Examples include $P2Y12^{-/-}$ mice and $CX3CR1^{gfp/gfp}$ mice [13, 54]. CSF1R is one microglia receptor involved in the proliferation and viability of microglia. Several selective CSF1R kinase inhibitors have been tested in disease models to pharmacologically eliminate microglia. PLX3397, for example, is a triple kinase inhibitor of CSF1R, c-Kit, and Flt3 [55, 56]. Blockages of CSF1R, c-Kit, and Flt3 by PLX3397, or PLX5622, administered for 2–5 weeks in the diet virtually eliminated microglia in the brain without causing cognitive or behavioral abnormalities, or obvious inflammation [57–60]. However, PLX3397 or PLX5622 induced global and chronic microglial ablation, which might limit the use of this approach in acute brain injury models to inhibit local microglial response.

Under pathologic conditions, the activated microglia accelerate disease progression by triggering secondary inflammatory injuries [12, 61]. Under physiologic conditions, compared to the microglial response after brain insults [62], the inflammatory response, after microglial elimination induced by Clo-Lip, is modest. Nevertheless, the similar outcomes between normal and pathologic microglial depletion with regards to microenvironmental changes in brain, and the synchronization of brain defense should be paid attention to.

To our knowledge, this study is the first to assess the status of neurons, astrocytes, and oligodendrocytes after acute microglial depletion by Clo-Lip in vivo under physiologic conditions. Although we evaluated only a limited number of histologic parameters in the acute period, our findings suggest that intracerebral application of Clo-Lip might alter the microenvironment in the brain after microglia are depleted. Our results highlight the need for caution when drawing conclusions about the dependent role of microglia in brain disease models.

Acknowledgments We thank Claire Levine for assistance with manuscript preparation.

Funding Information This work was supported by the National Institutes of Health (R01NS102583 and R01NS105894 to J. Wang), the American Heart Association (Grant-in-Aid 17GRNT33660766 to J. Wang; Scientist Development Grant 16SDG30980031 to X. Han; Postdoctoral

Fellowship Award 17POST33660191 to X. Lan), and a Stimulating and Advancing ACCM Research (StAAR) Award from the Department of Anesthesiology and Critical Care Medicine, Johns Hopkins University.

Compliance with Ethical Standards

Conflict of Interest The authors declare that they have no conflict of interest.

Ethical Approval All procedures performed in studies involving animals were in accordance with the ethical standards of the Johns Hopkins University, School of Medicine at which the studies were conducted.

Publisher's Note Springer Nature remains neutral with regard to jurisdictional claims in published maps and institutional affiliations.

References

1. Gatti D, Viapiana O, Idolazzi L, Fracassi E, Ionescu C, Dartizio C, Troplini S, Kunnathully V et al (2014) Distinct effect of zoledronate and clodronate on circulating levels of DKK1 and sclerostin in women with postmenopausal osteoporosis. Bone 67:189–192. https://doi.org/10.1016/j.bone.2014.06.037
2. Valenti MT, Mottes M, Biotti A, Perduca M, Pisani A, Bovi M, Deiana M, Cheri S et al (2017) Clodronate as a therapeutic strategy against osteoarthritis. Int J Mol Sci 18(12). https://doi.org/10.3390/ijms18122696
3. Frediani B, Bertoldi I (2015) Clodronate: new directions of use. Clin Cases Miner Bone Metab 12(2):97–108. https://doi.org/10.11138/ccmbm/2015.12.2.097
4. Nardi A, Ventura L, Cozzi L, Tonini G (2016) Clodronate news of efficacy in osteoporosis. Clin Cases Miner Bone Metab 13(1):33–35. https://doi.org/10.11138/ccmbm/2016.13.1.033
5. van Rooijen N, Hendrikx E (2010) Liposomes for specific depletion of macrophages from organs and tissues. Methods Mol Biol 605:189–203. https://doi.org/10.1007/978-1-60327-360-2_13
6. van Rooijen N, Sanders A, van den Berg TK (1996) Apoptosis of macrophages induced by liposome-mediated intracellular delivery of clodronate and propamidine. J Immunol Methods 193(1):93–99
7. Van Rooijen N, Sanders A (1994) Liposome mediated depletion of macrophages: mechanism of action, preparation of liposomes and applications. J Immunol Methods 174(1–2):83–93
8. Van Rooijen N, Sanders A (1996) Kupffer cell depletion by liposome-delivered drugs: comparative activity of intracellular clodronate, propamidine, and ethylenediaminetetraacetic acid. Hepatology 23(5):1239–1243. https://doi.org/10.1053/jhep.1996.v23.pm0008621159
9. Takano S, Uchida K, Inoue G, Miyagi M, Aikawa J, Iwase D, Iwabuchi K, Matsumoto T et al (2017) Nerve growth factor regulation and production by macrophages in osteoarthritic synovium. Clin Exp Immunol 190(2):235–243. https://doi.org/10.1111/cei.13007
10. Prinz M, Erny D, Hagemeyer N (2017) Ontogeny and homeostasis of CNS myeloid cells. Nat Immunol 18(4):385–392. https://doi.org/10.1038/ni.3703
11. Goldmann T, Wieghofer P, Jordao MJ, Prutek F, Hagemeyer N, Frenzel K, Amann L, Staszewski O et al (2016) Origin, fate and dynamics of macrophages at central nervous system interfaces. Nat Immunol 17(7):797–805. https://doi.org/10.1038/ni.3423
12. Lan X, Han X, Li Q, Yang QW, Wang J (2017) Modulators of microglial activation and polarization after intracerebral haemorrhage. Nat Rev Neurol 13(7):420–433. https://doi.org/10.1038/nrneurol.2017.69
13. Lou N, Takano T, Pei Y, Xavier AL, Goldman SA, Nedergaard M (2016) Purinergic receptor P2RY12-dependent microglial closure of the injured blood-brain barrier. Proc Natl Acad Sci U S A 113(4):1074–1079. https://doi.org/10.1073/pnas.1520398113
14. Miron VE, Boyd A, Zhao JW, Yuen TJ, Ruckh JM, Shadrach JL, van Wijngaarden P, Wagers AJ et al (2013) M2 microglia and macrophages drive oligodendrocyte differentiation during CNS remyelination. Nat Neurosci 16(9):1211–1218. https://doi.org/10.1038/nn.3469
15. Zhang Z, Zhang Z, Lu H, Yang Q, Wu H, Wang J (2017) Microglial polarization and inflammatory mediators after intracerebral hemorrhage. Mol Neurobiol 54(3):1874–1886. https://doi.org/10.1007/s12035-016-9785-6
16. Aguzzi A, Barres BA, Bennett ML (2013) Microglia: scapegoat, saboteur, or something else? Science 339(6116):156–161. https://doi.org/10.1126/science.1227901
17. Andreou KE, Soto MS, Allen D, Economopoulos V, de Bernardi A, Larkin JR, Sibson NR (2017) Anti-inflammatory microglia/macrophages as a potential therapeutic target in brain metastasis. Front Oncol 7:251. https://doi.org/10.3389/fonc.2017.00251
18. Fernandez-Lopez D, Faustino J, Klibanov AL, Derugin N, Blanchard E, Simon F, Leib SL, Vexler ZS (2016) Microglial cells prevent hemorrhage in neonatal focal arterial stroke. J Neurosci 36(10):2881–2893. https://doi.org/10.1523/JNEUROSCI.0140-15.2016
19. Faustino JV, Wang X, Johnson CE, Klibanov A, Derugin N, Wendland MF, Vexler ZS (2011) Microglial cells contribute to endogenous brain defenses after acute neonatal focal stroke. J Neurosci 31(36):12992–13001. https://doi.org/10.1523/JNEUROSCI.2102-11.2011
20. Hawkes CA, McLaurin J (2009) Selective targeting of perivascular macrophages for clearance of beta-amyloid in cerebral amyloid angiopathy. Proc Natl Acad Sci U S A 106(4):1261–1266. https://doi.org/10.1073/pnas.0805453106
21. Han X, Zhao X, Lan X, Li Q, Gao Y, Liu X, Wan J, Yang Z, et al. (2018) 20-HETE synthesis inhibition promotes cerebral protection after intracerebral hemorrhage without inhibiting angiogenesis. J Cereb Blood Flow Metab:271678X18762645. doi:https://doi.org/10.1177/0271678X18762645
22. Li Q, Wan J, Lan X, Han X, Wang Z, Wang J (2017) Neuroprotection of brain-permeable iron chelator VK-28 against intracerebral hemorrhage in mice. J Cereb Blood Flow Metab 37(9):3110–3123. https://doi.org/10.1177/0271678X17709186
23. Zhu W, Gao Y, Wan J, Lan X, Han X, Zhu S, Zang W, Chen X et al (2018) Changes in motor function, cognition, and emotion-related behavior after right hemispheric intracerebral hemorrhage in various brain regions of mouse. Brain Behav Immun 69:568–581. https://doi.org/10.1016/j.bbi.2018.02.004
24. Zhu W, Gao Y, Chang CF, Wan JR, Zhu SS, Wang J (2014) Mouse models of intracerebral hemorrhage in ventricle, cortex, and hippocampus by injections of autologous blood or collagenase. PLoS One 9(5):e97423. https://doi.org/10.1371/journal.pone.0097423
25. Yang J, Li Q, Wang Z, Qi C, Han X, Lan X, Wan J, Wang W et al (2017) Multimodality MRI assessment of grey and white matter injury and blood-brain barrier disruption after intracerebral haemorrhage in mice. Sci Rep 7:40358. https://doi.org/10.1038/srep40358
26. Li Q, Han X, Lan X, Gao Y, Wan J, Durham F, Cheng T, Yang J et al (2017) Inhibition of neuronal ferroptosis protects hemorrhagic brain. JCI Insight 2(7):e90777. https://doi.org/10.1172/jci.insight.90777
27. Lan X, Han X, Li Q, Li Q, Gao Y, Cheng T, Wan J, Zhu W et al (2017) Pinocembrin protects hemorrhagic brain primarily by inhibiting toll-like receptor 4 and reducing M1 phenotype

microglia. Brain Behav Immun 61:326–339. https://doi.org/10.1016/j.bbi.2016.12.012
28. Pierzchalski A, Mittag A, Bocsi J, Tarnok A (2013) An innovative cascade system for simultaneous separation of multiple cell types. PLoS One 8(9):e74745. https://doi.org/10.1371/journal.pone.0074745
29. Han X, Lan X, Li Q, Gao Y, Zhu W, Cheng T, Maruyama T, Wang J (2016) Inhibition of prostaglandin E2 receptor EP3 mitigates thrombin-induced brain injury. J Cereb Blood Flow Metab 36(6):1059–1074. https://doi.org/10.1177/0271678X15606462
30. Cheng T, Wang W, Li Q, Han X, Xing J, Qi C, Lan X, Wan J et al (2016) Cerebroprotection of flavanol (−)-epicatechin after traumatic brain injury via Nrf2-dependent and -independent pathways. Free Radic Biol Med 92:15–28. https://doi.org/10.1016/j.freeradbiomed.2015.12.027
31. Zhang J, Li X, Kwansa H, Kim YT, Yi L, Hong G, Andrabi SA, Dawson VL et al (2017) Augmentation of poly(ADP-ribose) polymerase-dependent neuronal cell death by acidosis. J Cereb Blood Flow Metab 37(6):1982–1993. https://doi.org/10.1177/0271678X16658491
32. Chung SJ, Nagaraju GP, Nagalingam A, Muniraj N, Kuppusamy P, Walker A, Woo J, Gyorffy B et al (2017) ADIPOQ/adiponectin induces cytotoxic autophagy in breast cancer cells through STK11/LKB1-mediated activation of the AMPK-ULK1 axis. Autophagy 13(8):1386–1403. https://doi.org/10.1080/15548627.2017.1332565
33. Cheng T, Yang B, Li D, Ma S, Tian Y, Qu R, Zhang W, Zhang Y et al (2015) Wharton's jelly transplantation improves neurologic function in a rat model of traumatic brain injury. Cell Mol Neurobiol 35(5):641–649. https://doi.org/10.1007/s10571-015-0159-9
34. Polfliet MM, Goede PH, van Kesteren-Hendrikx EM, van Rooijen N, Dijkstra CD, van den Berg TK (2001) A method for the selective depletion of perivascular and meningeal macrophages in the central nervous system. J Neuroimmunol 116(2):188–195
35. Huang Y, Xu Z, Xiong S, Sun F, Qin G, Hu G, Wang J, Zhao L et al (2018) Repopulated microglia are solely derived from the proliferation of residual microglia after acute depletion. Nat Neurosci 21(4):530–540. https://doi.org/10.1038/s41593-018-0090-8
36. Frith JC, Monkkonen J, Blackburn GM, Russell RG, Rogers MJ (1997) Clodronate and liposome-encapsulated clodronate are metabolized to a toxic ATP analog, adenosine 5′-(beta, gamma-dichloromethylene) triphosphate, by mammalian cells in vitro. J Bone Miner Res 12(9):1358–1367. https://doi.org/10.1359/jbmr.1997.12.9.1358
37. Lehenkari PP, Kellinsalmi M, Napankangas JP, Ylitalo KV, Monkkonen J, Rogers MJ, Azhayev A, Vaananen HK et al (2002) Further insight into mechanism of action of clodronate: inhibition of mitochondrial ADP/ATP translocase by a nonhydrolyzable, adenine-containing metabolite. Mol Pharmacol 61(5):1255–1262
38. Nixon RA, Cataldo AM (1995) The endosomal-lysosomal system of neurons: new roles. Trends Neurosci 18(11):489–496
39. Ferguson SM (2018) Neuronal lysosomes. Neurosci Lett. https://doi.org/10.1016/j.neulet.2018.04.005
40. Gorenstein C, Bundman MC, Lew PJ, Olds JL, Ribak CE (1985) Dendritic transport. I. Colchicine stimulates the transport of lysosomal enzymes from cell bodies to dendrites. J Neurosci 5(8):2009–2017
41. Ehlers MD (2000) Reinsertion or degradation of AMPA receptors determined by activity-dependent endocytic sorting. Neuron 28(2):511–525
42. Fernandez-Monreal M, Brown TC, Royo M, Esteban JA (2012) The balance between receptor recycling and trafficking toward lysosomes determines synaptic strength during long-term depression. J Neurosci 32(38):13200–13205. https://doi.org/10.1523/JNEUROSCI.0061-12.2012
43. Gowrishankar S, Yuan P, Wu Y, Schrag M, Paradise S, Grutzendler J, De Camilli P, Ferguson SM (2015) Massive accumulation of luminal protease-deficient axonal lysosomes at Alzheimer's disease amyloid plaques. Proc Natl Acad Sci U S A 112(28):E3699–E3708. https://doi.org/10.1073/pnas.1510329112
44. Blazquez-Llorca L, Valero-Freitag S, Rodrigues EF, Merchan-Perez A, Rodriguez JR, Dorostkar MM, DeFelipe J, Herms J (2017) High plasticity of axonal pathology in Alzheimer's disease mouse models. Acta Neuropathol Commun 5(1):14. https://doi.org/10.1186/s40478-017-0415-y
45. Rangaraju V, Calloway N, Ryan TA (2014) Activity-driven local ATP synthesis is required for synaptic function. Cell 156(4):825–835. https://doi.org/10.1016/j.cell.2013.12.042
46. Fernandez-Lopez D, Faustino J, Daneman R, Zhou L, Lee SY, Derugin N, Wendland MF, Vexler ZS (2012) Blood-brain barrier permeability is increased after acute adult stroke but not neonatal stroke in the rat. J Neurosci 32(28):9588–9600. https://doi.org/10.1523/JNEUROSCI.5977-11.2012
47. Biname F, Sakry D, Dimou L, Jolivel V, Trotter J (2013) NG2 regulates directional migration of oligodendrocyte precursor cells via Rho GTPases and polarity complex proteins. J Neurosci 33(26):10858–10874. https://doi.org/10.1523/JNEUROSCI.5010-12.2013
48. Kucharova K, Stallcup WB (2015) NG2-proteoglycan-dependent contributions of oligodendrocyte progenitors and myeloid cells to myelin damage and repair. J Neuroinflammation 12:161. https://doi.org/10.1186/s12974-015-0385-6
49. Xiang P, Zhu L, Jiang H, He BP (2015) The activation of NG2 expressing cells is downstream to microglial reaction and mediated by the transforming growth factor beta 1. J Neuroimmunol 279:50–63. https://doi.org/10.1016/j.jneuroim.2015.01.006
50. Hackett AR, Yahn SL, Lyapichev K, Dajnoki A, Lee DH, Rodriguez M, Cammer N, Pak J et al (2018) Injury type-dependent differentiation of NG2 glia into heterogeneous astrocytes. Exp Neurol 308:72–79. https://doi.org/10.1016/j.expneurol.2018.07.001
51. Sugimoto K, Nishioka R, Ikeda A, Mise A, Takahashi H, Yano H, Kumon Y, Ohnishi T et al (2014) Activated microglia in a rat stroke model express NG2 proteoglycan in peri-infarct tissue through the involvement of TGF-beta1. Glia 62(2):185–198. https://doi.org/10.1002/glia.22598
52. Kumamaru H, Saiwai H, Kobayakawa K, Kubota K, van Rooijen N, Inoue K, Iwamoto Y, Okada S (2012) Liposomal clodronate selectively eliminates microglia from primary astrocyte cultures. J Neuroinflammation 9:116. https://doi.org/10.1186/1742-2094-9-116
53. Ji K, Akgul G, Wollmuth LP, Tsirka SE (2013) Microglia actively regulate the number of functional synapses. PLoS One 8(2):e56293. https://doi.org/10.1371/journal.pone.0056293
54. Zanier ER, Marchesi F, Ortolano F, Perego C, Arabian M, Zoerle T, Sammali E, Pischiutta F et al (2016) Fractalkine receptor deficiency is associated with early protection but late worsening of outcome following brain trauma in mice. J Neurotrauma 33(11):1060–1072. https://doi.org/10.1089/neu.2015.4041
55. Dagher NN, Najafi AR, Kayala KM, Elmore MR, White TE, Medeiros R, West BL, Green KN (2015) Colony-stimulating factor 1 receptor inhibition prevents microglial plaque association and improves cognition in 3xTg-AD mice. J Neuroinflammation 12:139. https://doi.org/10.1186/s12974-015-0366-9
56. Tap WD, Wainberg ZA, Anthony SP, Ibrahim PN, Zhang C, Healey JH, Chmielowski B, Staddon AP et al (2015) Structure-guided blockade of CSF1R kinase in tenosynovial giant-cell tumor. N Engl J Med 373(5):428–437. https://doi.org/10.1056/NEJMoa1411366

57. Elmore MR, Najafi AR, Koike MA, Dagher NN, Spangenberg EE, Rice RA, Kitazawa M, Matusow B et al (2014) Colony-stimulating factor 1 receptor signaling is necessary for microglia viability, unmasking a microglia progenitor cell in the adult brain. Neuron 82(2):380–397. https://doi.org/10.1016/j.neuron.2014.02.040
58. Elmore MR, Lee RJ, West BL, Green KN (2015) Characterizing newly repopulated microglia in the adult mouse: impacts on animal behavior, cell morphology, and neuroinflammation. PLoS One 10(4):e0122912. https://doi.org/10.1371/journal.pone.0122912
59. Janova H, Arinrad S, Balmuth E, Mitjans M, Hertel J, Habes M, Bittner RA, Pan H et al (2018) Microglia ablation alleviates myelin-associated catatonic signs in mice. J Clin Invest 128(2):734–745. https://doi.org/10.1172/JCI97032
60. Hilla AM, Diekmann H, Fischer D (2017) Microglia are irrelevant for neuronal degeneration and axon regeneration after acute injury. J Neurosci 37(25):6113–6124. https://doi.org/10.1523/JNEUROSCI.0584-17.2017
61. Lan X, Han X, Liu X, Wang J (2018) Inflammatory responses after intracerebral hemorrhage: from cellular function to therapeutic targets. J Cereb Blood Flow Metab:271678X18805675. doi:https://doi.org/10.1177/0271678X18805675
62. Chang CF, Wan J, Li Q, Renfroe SC, Heller NM, Wang J (2017) Alternative activation-skewed microglia/macrophages promote hematoma resolution in experimental intracerebral hemorrhage. Neurobiol Dis 103:54–69. https://doi.org/10.1016/j.nbd.2017.03.016